

# Roles of N-Terminal Region Residues Lys11, Arg13, and Arg24 of Antithrombin in Heparin Recognition and in Promotion and Stabilization of the Heparin-Induced Conformational Change<sup>†</sup>

Sophia Schedin-Weiss,<sup>‡</sup> Umesh R. Desai,<sup>§,||</sup> Susan C. Bock,<sup>⊥</sup> Steven T. Olson,<sup>§</sup> and Ingemar Björk<sup>\*,‡</sup>

Department of Molecular Biosciences, Swedish University of Agricultural Sciences, Uppsala Biomedical Center, SE-751 23 Uppsala, Sweden, Center for Molecular Biology of Oral Diseases, University of Illinois—Chicago, Chicago, Illinois 60612, Department of Medicinal Chemistry, Virginia Commonwealth University, Richmond, Virginia 23298, and Departments of Medicine and Bioengineering, University of Utah Health Sciences Center—Pulmonary Division, University of Utah, Salt Lake City, Utah 84132

Received July 23, 2003

**ABSTRACT:** The N-terminal region residues, Lys11, Arg13, and Arg24, of the plasma coagulation inhibitor, antithrombin, have been implicated in binding of the anticoagulant polysaccharide, heparin, from the identification of natural mutants with impaired heparin binding or by the X-ray structure of a complex of the inhibitor with a high-affinity heparin pentasaccharide. Mutations of Lys11 or Arg24 to Ala in this work each reduced the affinity for the pentasaccharide ~40-fold, whereas mutation of Arg13 to Ala led to a decrease of only ~7-fold. All three substitutions resulted in the loss of one ionic interaction with the pentasaccharide and those of Lys11 or Arg24 also in 3–5-fold losses in affinity of nonionic interactions. Only the mutation of Lys11 affected the initial, weak interaction step of pentasaccharide binding, decreasing the affinity of this step ~2-fold. The mutations of Lys11 and Arg13 moderately, 2–7-fold, altered both rate constants of the second, conformational change step, whereas the substitution of Arg24 appreciably, ~25-fold, reduced the reverse rate constant of this step. The N-terminal region of antithrombin is thus critical for high-affinity heparin binding, Lys11 and Arg24 being responsible for maintaining appreciable and comparable binding energy, whereas Arg13 is less important. Lys11 is the only one of the three residues that is involved in the initial recognition step, whereas all three residues participate in the conformational change step. Lys11 and Arg13 presumably bind directly to the heparin pentasaccharide by ionic, and in the case of Lys11, also nonionic interactions. However, the role of Arg24 most likely is indirect, to stabilize the heparin-induced P-helix by interacting intramolecularly with Glu113 and Asp117, thereby positioning the crucial Lys114 residue for optimal ionic and nonionic interactions with the pentasaccharide. Together, these findings show that N-terminal residues of antithrombin make markedly different contributions to the energetics and dynamics of binding of the pentasaccharide ligand to the native and activated conformational states of the inhibitor that could not have been predicted from the X-ray structure.

Antithrombin is a vital plasma regulator of blood clotting (1). It is a proteinase inhibitor of the serpin superfamily, whose main targets are blood clotting proteinases, primarily thrombin, factor Xa, and factor IXa (2–6). Proteins of the serpin family share some typical structural features, most prominently a large, five-stranded  $\beta$ -sheet ( $\beta$ -sheet A) and a surface-exposed loop containing the reactive bond (2, 7). Serpins irreversibly inhibit their target proteinases by a

unique conformational change mechanism. The proteinase initially recognizes and processes the reactive bond of the serpin to the acyl-intermediate stage, as in a normal substrate. However, at this stage, the N-terminal part of the severed reactive-bond loop inserts as a new strand in the middle of  $\beta$ -sheet A, dragging the covalently attached proteinase along the surface to the opposite pole of the serpin. As a result, the proteinase is inactivated through compression against the body of the serpin, leading to distortion of its active site (3, 7–11).

The rate by which antithrombin inactivates its target proteinases can be enhanced up to several 1000-fold by the sulfated glycosaminoglycan heparin, due to two different mechanisms. A conformational change induced by binding of a specific pentasaccharide sequence within the heparin chain allosterically activates the inhibitor, thereby increasing the inhibition rate. Moreover, a bridging effect by which heparin brings antithrombin and the proteinase into a ternary complex further increases this rate (2, 3, 12). The individual

<sup>†</sup> This work was supported by grants from the Swedish Scientific Council—Medicine and the GLIBS program of the Foundation for Strategic Research (I.B.), by National Institutes of Health Grants HL30712 (S.C.B.) and HL39888 (S.T.O.), and by grants from American Heart Association of Metropolitan Chicago and American Heart Association—Mid-Atlantic Affiliate (U.R.D.).

\* To whom correspondence should be addressed. Tel: +46 18 4714191. Fax: +46 18 550762. E-mail: Ingemar.Bjork@vmk.slu.se.

<sup>‡</sup> Swedish University of Agricultural Sciences.

<sup>§</sup> University of Illinois—Chicago.

<sup>||</sup> Virginia Commonwealth University.

<sup>⊥</sup> University of Utah.

contributions of these two mechanisms to heparin acceleration of antithrombin inhibition vary for different proteinases, the conformational change being of major importance for factors Xa and IXa and the bridging effect dominating for thrombin. Binding of the heparin pentasaccharide occurs in two steps. An initial weak complex is first formed, followed by the conformational change in the second step (13–16). The X-ray structures of antithrombin and its complex with a synthetic variant of the heparin pentasaccharide (17, 18) indicate that this change involves elongation of the A- and D-helices, formation of the new short P-helix at the base of the D-helix, and contraction of the A-sheet. These changes lead to a higher accessibility of the reactive bond and exposure of exosites surrounding the loop, thus promoting the binding of target proteinases (19, 20).

Studies of natural and recombinant antithrombin variants, as well as the X-ray structure of free antithrombin and the antithrombin–pentasaccharide complex, have revealed the region of antithrombin to which the heparin pentasaccharide binds with high affinity and specificity (reviewed in ref 5). This region consists primarily of positively charged lysines and arginines within the A- and D-helices and the N-terminal region of antithrombin, including Lys11, Arg13, Arg46, Arg47, Lys114, Lys125, and Arg129. The contributions of Arg46 and Arg47, located in the A-helix, and of Lys114, Lys125, and Arg129 within the D- and P-helices to heparin binding have been extensively examined. The latter three residues contribute most of the binding energy and apparently act cooperatively in the binding mechanism (21–25).

Because of its accelerating effect on antithrombin inhibition of blood clotting proteinases, heparin is frequently used for the prevention of venous thromboembolism. Recent clinical trials have shown that the synthetic pentasaccharide is even more effective for this purpose than the previously used heparin forms (26–28). Nevertheless, the physiological role of heparin in activating the anticoagulant activity of antithrombin remains controversial (29), although heparin-like glycosaminoglycans on the vessel wall have been suggested to be endogenous antithrombin activators (30, 31). However, congenital mutations causing a heparin binding defect in human antithrombin support a biological role of the interaction, as individuals homozygous for such defects suffer an increased risk of developing thrombosis (4).

From the identification of a natural human mutant with a heparin binding defect, Arg24 was originally proposed to be directly involved in heparin binding (32). However, Arg24 was found not to be in close enough proximity to the pentasaccharide in the crystal structure of the complex to establish any interaction (18). The aim of the present work was to resolve this apparent discrepancy and also to clarify the contributions of the adjacent N-terminal region residues, Lys11 and Arg13, to heparin binding. Although these latter residues have been implicated to interact with the pentasaccharide by the X-ray structure of the complex (18), their individual roles in the binding have not been established. To address these questions, we introduced mutations of Lys11 to Ala or His, Arg13 to Ala, and Arg24 to Ala and characterized the effects on the affinity and kinetics of heparin binding. We found that Lys11 contributes substantially to the affinity by establishing ionic and nonionic interactions, presumably directly with the pentasaccharide,

and by participating in both steps of the binding mechanism. Arg13 contributes less affinity and only by making ionic interactions, also presumably directly with the pentasaccharide, in the second step. Arg24 is also of appreciable importance in the second binding step by stabilizing the activated state of the inhibitor, although most likely not by directly binding to the pentasaccharide but by forming intramolecular interactions with Glu113 and Asp117, located in the pentasaccharide-induced P-helix.

## MATERIALS AND METHODS

**Antithrombin Variants.** Recombinant antithrombin variants with Lys11 to Ala, Lys11 to His, Arg13 to Ala, and Arg24 to Ala substitutions were produced by site-directed mutagenesis, expressed in a baculovirus system on an Asn135Ala background, and purified by heparin affinity chromatography as described previously (21, 22, 33–35). Certain preparations required further purification by anion-exchange chromatography on a MonoQ HR 5/5 column (Amersham Pharmacia Biotech) (23).

The purity of the antithrombin preparations was assessed by SDS–PAGE with the Tris/glycine or Tris/Tricine buffer systems (36, 37) and by PAGE under nondenaturing conditions with the Tris/glycine buffer system. Protein concentrations of the antithrombin variants were determined by absorbance measurements at 280 nm from a molar absorption coefficient of  $37\,700\text{ M}^{-1}\text{ cm}^{-1}$  (38).

**Proteinases and Saccharides.** Human  $\alpha$ -thrombin was a gift from Dr. John Fenton (New York State Department of Health, Albany, NY). Human factor Xa was prepared as described previously (39). The concentrations of the enzymes were based on active-site titrations, in which thrombin and factor Xa were shown to be >90% and >70% active, respectively.

The synthetic antithrombin binding heparin pentasaccharide (40) was a gift from Dr. M. Petitou (Sanofi Recherche, Toulouse, France). Full-length heparin with high affinity for antithrombin and with an average molecular mass of  $\sim 8000$  Da (i.e., comprising  $\sim 26$  saccharide units) was isolated from commercial heparin (14, 41, 42). Concentrations of the two saccharides were determined by stoichiometric fluorescence titrations with plasma antithrombin (14, 42).

**Experimental Conditions.** All experiments were performed at  $25 \pm 0.2^\circ\text{C}$  and pH 7.4 or 6.0 in 20 mM sodium phosphate buffer containing 0.1 mM EDTA and 0.1% poly(ethylene glycol) 8000. The ionic strength of this buffer in the absence of added salt is 0.05 and 0.025 at the two pH values, respectively, and NaCl was added to final ionic strengths of up to 0.7.

**Stoichiometries and Affinities of Heparin Binding.** Stoichiometries and dissociation equilibrium constants,  $K_d$ ,<sup>1</sup> for the binding of pentasaccharide or full-length heparin to the antithrombin variants were measured by titrations, monitored

<sup>1</sup> Abbreviations: H26, full-length heparin with a high affinity for antithrombin and containing  $\sim 26$  saccharide units; H5, antithrombin binding heparin pentasaccharide;  $K_d$ , dissociation equilibrium constant;  $k_{\text{obs}}$ , observed pseudo-first-order rate constant;  $k_{\text{on}}$ , overall association rate constant;  $k_{\text{off}}$ , overall dissociation rate constant; K11A and K11H, substitution of Lys11 by Ala and His, respectively; R13A and R24A, substitution of Arg13 and Arg24, respectively, by Ala; N135A, substitution of Asn135 by Ala; PAGE, polyacrylamide gel electrophoresis; SDS, sodium dodecyl sulfate.

by the fluorescence enhancement induced by the interaction, of the variants with the saccharides, as described previously (14, 41, 42). Stoichiometric titrations were performed at pH 7.4 and ionic strengths 0.1 or 0.15 with full-length heparin and with antithrombin concentrations, based on absorbance measurements, at least 20-fold above  $K_d$ . Affinity titrations were done at pH 7.4 or 6.0 and ionic strengths 0.1–0.7 with pentasaccharide or full-length heparin and with concentrations of active antithrombin 2-fold below to 4-fold above  $K_d$ . The measurements were made in an SLM 4800S or 8000C spectrofluorometer (SLM Instruments, Rochester, NY) with excitation and emission wavelengths of 280 and 340 nm, respectively. The data were fitted to the equilibrium binding equation by nonlinear least-squares regression (42).

**Kinetics of Heparin Binding.** The rates of binding of pentasaccharide or full-length heparin to the antithrombin variants were determined at pH 7.4 and ionic strengths 0.15 or 0.3 in a stopped-flow instrument (SX-17MV; Applied Biophysics, Leatherhead, UK) by monitoring the fluorescence increase induced by the saccharides, as described earlier (14, 15, 35). The fluorescence was measured with an excitation wavelength of 280 nm and an emission cutoff filter with ~50% transmission at 320 nm. The experiments were done under pseudo-first-order conditions (i.e., with heparin concentrations  $\geq 5$ -fold, and in most cases  $\geq 10$ -fold, higher than concentrations of active antithrombin). Observed pseudo-first-order rate constants,  $k_{\text{obs}}$ , were obtained by nonlinear regression fitting of the progress curves to a single exponential function. Approximately 16 fluorescence traces were averaged for each rate constant determination.

**Stoichiometries and Kinetics of Proteinase Inactivation.** Stoichiometries of inhibition of human thrombin by the antithrombin variants were measured essentially as in previous work (21, 22, 35). A series of samples of thrombin at a constant concentration of 0.1 or 0.5  $\mu\text{M}$  was incubated for 4–20 h (for 0.1  $\mu\text{M}$  thrombin) or 1–2 h (for 0.5  $\mu\text{M}$  thrombin) with increasing concentrations of antithrombin, based on absorbance measurements, at pH 7.4 and ionic strength 0.15. The residual activity of the enzyme was then determined from the initial rate of hydrolysis of the substrate, S2238 (Chromogenix, Mölndal, Sweden), monitored as the increase of absorbance at 405 nm. The inhibition stoichiometries were derived from the intercept on the abscissa of plots of the residual enzyme activity versus the molar ratio of antithrombin to proteinase (42).

Second-order association rate constants for inhibition of human thrombin or factor Xa by the antithrombin variants in the absence or presence of pentasaccharide or full-length heparin were determined under pseudo-first-order conditions at pH 7.4 and ionic strength 0.15 (21, 22, 35, 42). Reactions were done with 70–200 nM active antithrombin, 10 nM proteinase, and 0–8 nM pentasaccharide or full-length heparin. After various times, portions of the reaction mixture were quenched by dilution into 100  $\mu\text{M}$  of the substrates, S2238 for thrombin or Spectrozyme FXa (American Diagnostica, Greenwich, CT) for factor Xa. The residual enzyme activity was determined from the initial rate of substrate hydrolysis, monitored by absorbance measurements at 405 nm. Observed pseudo-first-order rate constants,  $k_{\text{obs}}$ , were obtained by fitting the time-dependence of the loss of enzyme activity to a single-exponential function with an end-point of zero activity (42). Second-order association rate constants

for uncatalyzed reactions were obtained by dividing  $k_{\text{obs}}$  by the inhibitor concentration, whereas those for pentasaccharide- or full-length heparin-catalyzed reactions were determined from the slope of linear regression fits of the dependence of  $k_{\text{obs}}$  on the concentration of the antithrombin–saccharide complex (35, 43).

## RESULTS

**Purification and Characterization of Antithrombin Variants.** Antithrombin with an Asn135 to Ala mutation was used as a base molecule for additional substitutions of Lys11 to Ala, Lys11 to His, Arg13 to Ala, and Arg24 to Ala in this paper. The N135A substitution was introduced because it prevents glycosylation of the Asn135 site and thus circumvents the heparin binding heterogeneity caused by incomplete glycosylation at this site (33, 35, 44). The N135A variant resembles the  $\beta$ -form of antithrombin in plasma, which also lacks an oligosaccharide side chain at Asn135 and has a higher heparin affinity than the predominant  $\alpha$ -form, as the oligosaccharide at this site in  $\alpha$ -antithrombin sterically hinders heparin binding (33, 35). The baculovirus expression system was used in this study because it introduces shorter and structurally less divergent oligosaccharide chains than mammalian expression systems to the remaining three glycosylation sites and therefore further decreases heparin binding heterogeneity (33, 45, 46). Most preparations of the antithrombin variants could be purified to acceptable homogeneity by heparin affinity chromatography. However, the K11H/N135A variant and some preparations of the R13A/N135A and R24A/N135A variants required further purification by anion exchange chromatography. All final antithrombin preparations used were  $>95\%$  homogeneous in SDS–PAGE and nondenaturing PAGE. The K11A/N135A, K11H/N135A, R13A/N135A, and R24A/N135A variants showed a slightly higher mobility than the N135A control in nondenaturing PAGE, consistent with the loss of a positive charge.

The stoichiometry of binding of full-length heparin to the variants was 0.8 for the K11A/N135A variant, 0.8 for the K11H/N135A variant, 0.75 for the R13A/N135A variant, and varied between 0.6 and 0.8 for the different preparations of the R24A/N135A variant used. The corresponding stoichiometries of thrombin binding were comparable with those of heparin binding, being 0.8, 0.9, 0.7, and 0.6–0.8 for the K11A/N135A, K11H/N135A, R13A/N135A, and R24A/N135A variants, respectively. The preparations thus contained some inactive, presumably latent, form of the inhibitor, as also seen in previous studies with other recombinant antithrombin variants (21–25, 35). All subsequent analyses of heparin binding or proteinase inhibition by the variants were based on concentrations of active protein. All four variants showed a normal 30–40% increase in tryptophan fluorescence in the heparin stoichiometry titrations.

**Affinity of Pentasaccharide and Full-Length Heparin Binding.** Dissociation equilibrium constants,  $K_d$ , for the interaction of the pentasaccharide with most of the antithrombin variants at pH 7.4 and ionic strengths 0.15 and 0.3 were measured by fluorescence titrations. However, the affinities of the pentasaccharide for the N135A and R13A/N135A variants at ionic strength 0.15 were too high to be measured directly with good precision but were instead



Table 1: Dissociation Equilibrium Constants, Bimolecular Association Rate Constants, and Dissociation Rate Constants for Pentasaccharide and Full-Length Heparin Binding to the N135A, K11A/N135A, K11H/N135A, R13A/N135A, and R24A/N135A Antithrombin Variants at 25 °C, pH 7.4 and Ionic Strengths 0.15 and 0.3<sup>a</sup>

ionic strength	heparin form	antithrombin variant	$K_d$ (nM)	$k_{on}$ ( $\times 10^6 M^{-1} s^{-1}$ )	$k_{off}$ ( $s^{-1}$ )	calculated $K_d$ (nM) <sup>b</sup>	calculated $k_{off}$ ( $s^{-1}$ ) <sup>c</sup>
0.15	H5	N135A	$2 \pm 1^{d,e}$	$70 \pm 2^e$	nd <sup>f</sup>		$0.14 \pm 0.07^e$
		K11A/N135A	$79 \pm 8$	$12 \pm 0.4$	$1.9 \pm 0.3$	$150 \pm 30$	$0.95 \pm 0.1$
		K11H/N135A	$12 \pm 2$	$28 \pm 0.6$	$0.2 \pm 0.5$	$7 \pm 18$	$0.34 \pm 0.06$
		R13A/N135A	$15 \pm 5^d$	$23 \pm 0.6$	$1.0 \pm 0.4$	$43 \pm 18$	$0.3 \pm 0.1$
		R24A/N135A	$86 \pm 4$	$37 \pm 2$	$4.4 \pm 1.3$	$120 \pm 40$	$3.2 \pm 0.3$
0.3	H5	N135A	$40 \pm 4^e$	$28 \pm 1^e$	$1.5 \pm 0.4^e$	$54 \pm 16^e$	$1.1 \pm 0.1^e$
		K11A/N135A	$720 \pm 23$	$3.8 \pm 0.3$	$3.8 \pm 0.3$	$1000 \pm 200$	$2.7 \pm 0.1$
		K11H/N135A	$160 \pm 18$	$8.3 \pm 0.1$	$1.5 \pm 0.1$	$180 \pm 10$	$1.3 \pm 0.2$
		R13A/N135A	$160 \pm 11$	$8.3 \pm 0.3$	$2.8 \pm 0.2$	$340 \pm 40$	$1.3 \pm 0.1$
		R24A/N135A	$950 \pm 40$	$12 \pm 0.4$	$15 \pm 0.8$	$1200 \pm 100$	$11 \pm 0.8$
	H26	N135A	$7 \pm 1^e$	$23 \pm 0.2^e$	$0.3 \pm 0.1^e$	$13 \pm 4^e$	$0.16 \pm 0.02^e$
		K11A/N135A	$200 \pm 11$	$3.8 \pm 0.1$	$0.51 \pm 0.05$	$130 \pm 20$	$0.78 \pm 0.06$
		K11H/N135A	$61 \pm 1$	$6.6 \pm 0.3$	$0.31 \pm 0.15$	$47 \pm 25$	$0.40 \pm 0.02$
		R13A/N135A	$36 \pm 3$	$9.0 \pm 0.1$	$0.5 \pm 0.1$	$56 \pm 12$	$0.3 \pm 0.03$
		R24A/N135A	$260 \pm 8$	$9.5 \pm 0.1$	$4.4 \pm 0.1$	$460 \pm 15$	$2.5 \pm 0.1$

<sup>a</sup> Measured  $K_d$  values are averages of two to six fluorescence titrations. Errors are  $\pm$ SEM for three or more titrations and range for two titrations. Measured values of  $k_{on}$  and  $k_{off} \pm$  SEM were obtained by linear regression of plots of  $k_{obs}$  vs heparin concentration comprising five to seven points in the 0.2–2.6  $\mu$ M concentration range. <sup>b</sup> From  $k_{on}$  and  $k_{off}$ . <sup>c</sup> From  $k_{on}$  and  $K_d$ . <sup>d</sup> Obtained by linear extrapolation of values measured at higher ionic strengths. <sup>e</sup> Taken from ref 21. <sup>f</sup> Not determined.

obtained by extrapolation of values measured at higher ionic strengths (see next). Dissociation equilibrium constants for the interaction of full-length heparin with the variants were only measured at pH 7.4, ionic strength 0.3, as the interaction at ionic strength 0.15 was too tight for the data to allow any reasonable interpretation. Full-length heparin bound between  $\sim$ 3- and  $\sim$ 6-fold tighter than the pentasaccharide to all variants (Table 1), an affinity difference comparable with that seen in previous studies with wild-type antithrombin and other antithrombin variants (14, 21–25, 35, 47). The K11A, K11H, R13A, and R24A substitutions all resulted in a reduced heparin affinity (Table 1). The K11A/N135A and R24A/N135A variants both bound the pentasaccharide appreciably,  $\sim$ 40-fold, more weakly than the N135A control at ionic strength 0.15, whereas the corresponding affinity loss shown by the R13A/N135A variant was lower,  $\sim$ 7-fold. The affinity of the K11H/N135A variant for the pentasaccharide at ionic strength 0.15, although  $\sim$ 6-fold lower than that of the control, was notably higher than that of the K11A/N135A variant. The affinity losses for the pentasaccharide at ionic strength 0.3 were slightly, up to 2-fold, smaller than at ionic strength 0.15 for all variants, due to the reduction in the number of ionic interactions caused by the mutations altering the dependence of  $K_d$  on sodium ion concentration, as compared with that of the control (see next). The decreases in antithrombin affinity for full-length heparin at ionic strength 0.3 caused by the substitutions were comparable with the reductions in affinity for the pentasaccharide.

**Ionic and Nonionic Contributions to Pentasaccharide Binding.** The ionic and nonionic contributions to the losses of antithrombin affinity for the pentasaccharide at pH 7.4 caused by the K11A, K11H, R13A, and R24A substitutions were determined from the dependence of the dissociation equilibrium constants on sodium ion concentration. Plots of  $\log K_d$  versus  $\log [Na^+]$  were linear for all antithrombin variants (Figure 1). Polyelectrolyte theory (14, 35, 41, 48) states that the slope of such plots is equal to  $Z\Psi$ , where  $Z$  represents the number of charge–charge interactions involved in the binding, and  $\Psi$  is the number of sodium ions

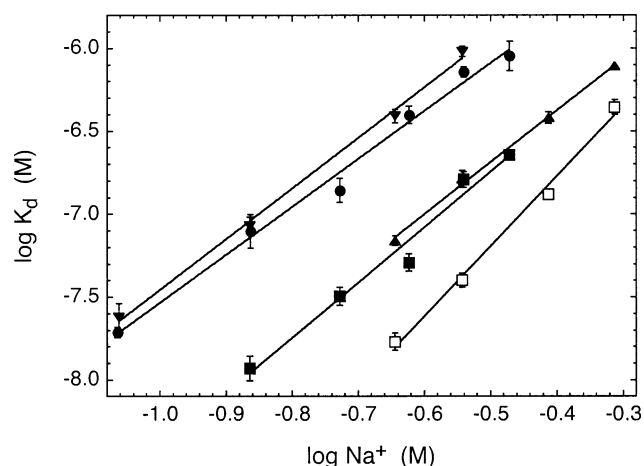


FIGURE 1: Sodium ion concentration dependence of dissociation equilibrium constants for pentasaccharide binding to the N135A, K11A/N135A, K11H/N135A, R13A/N135A, and R24A/N135A antithrombin variants at 25 °C, pH 7.4. (□) N135A; (●) K11A/N135A; (■) K11H/N135A; (▲) R13A/N135A; and (▼) R24A/N135A. Each value represents the average  $\pm$  SEM of three to six determinations. Error bars not shown lie within the dimensions of the symbols. The solid lines represent linear regression fits. The data for N135A are taken from ref 21.

bound per heparin charge that are released upon heparin binding [estimated to 0.8 (41)]. Moreover, the ordinate intercept,  $\log K_d'$  (i.e.,  $\log K_d$  at 1 M NaCl), of the plots represents the nonionic contribution to heparin binding. The N135A control variant makes  $\sim$ 5 ionic interactions with the pentasaccharide (21, 35), whereas the K11A/N135A, K11H/N135A, R13A/N135A, and R24A/N135A variants all made  $\sim$ 4 ionic interactions, in consideration of the errors of the measurements (Table 2). Each substitution thus caused the loss of  $\sim$ 1 ionic interaction, consistent with the loss of one positive charge. In addition,  $\log K_d'$  was increased from  $-5.1$  for the N135A control to  $-4.6$  for the K11A/N135A variant and to  $-4.4$  for the R24A/N135A variant (Table 2), corresponding to  $\sim$ 3- and  $\sim$ 5-fold losses in affinity of nonionic interactions, respectively, for the two variants. In

Table 2: Ionic and Nonionic Contributions to Pentasaccharide Binding to the N135A, K11A/N135A, K11H/N135A, R13A/N135A, and R24A/N135A Antithrombin Variants at 25 °C, pH 7.4 and 6.0<sup>a</sup>

pH	antithrombin variant	Z	log( $K_d'$ )	$K_d'$ ( $\mu$ M)
7.4	N135A	5.3 $\pm$ 0.2 <sup>b</sup>	-5.1 $\pm$ 0.1 <sup>b</sup>	8 $\pm$ 2
	K11A/N135A	3.6 $\pm$ 0.2	-4.6 $\pm$ 0.1	25 $\pm$ 6
	K11H/N135A	4.2 $\pm$ 0.4	-5.1 $\pm$ 0.2	8 $\pm$ 4
	R13A/N135A	3.9 $\pm$ 0.1	-5.1 $\pm$ 0.05	8 $\pm$ 1
	R24A/N135A	3.8 $\pm$ 0.1	-4.4 $\pm$ 0.1	40 $\pm$ 9
6.0	N135A	6.1 $\pm$ 0.3 <sup>c</sup>	-5.9 $\pm$ 0.1 <sup>c</sup>	1.3 $\pm$ 0.3
	K11H/N135A	5.9 $\pm$ 0.2	-6.2 $\pm$ 0.1	0.6 $\pm$ 0.1

<sup>a</sup> The ionic (Z) and nonionic (log  $K_d'$ ) contributions to pentasaccharide binding were determined from the slopes and intercepts, respectively, of plots of log( $K_d'$ ) vs log [Na<sup>+</sup>] (Figure 1 and similar plots, not shown, at pH 6.0), as described in the Results. Errors represent the SEM obtained by linear regression. <sup>b</sup> Taken from ref 21. <sup>c</sup> Taken from ref 22.

contrast, log  $K_d'$  for the K11H/N135A and R13A/N135A variants was the same as that of the control. The K11A and R24A mutations thus each caused losses of both one ionic interaction and nonionic interactions, whereas the K11H and R13A mutations each caused the loss of essentially only one ionic interaction.

The dependence of  $K_d$  for pentasaccharide binding to the K11H/N135A variant on sodium ion concentration was also assessed at pH 6.0. No differences in either the number of ionic interactions made or the affinity of the nonionic interactions from the values of the N135A control were evident at this pH (Table 2). The ionic interaction indicated by the data to be lost at pH 7.4 was thus apparently regained at pH 6.0, where His is positively charged. Moreover, the results at pH 6.0 support the conclusion that the K11H substitution did not lead to any loss of nonionic interactions.

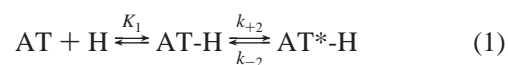
**Kinetics of Heparin Binding.** The kinetics of pentasaccharide or full-length heparin binding to the antithrombin variants at pH 7.4 and ionic strengths of 0.15 or 0.3 were evaluated under pseudo-first-order conditions in a stopped-flow instrument by monitoring the increase in tryptophan fluorescence induced by the interaction. The fluorescence change could be well-fitted to a single-exponential function for all interactions studied. The dependence of the observed pseudo-first-order rate constant,  $k_{\text{obs}}$ , obtained from these fits on saccharide concentration was linear in the low concentration range (from 0.2  $\mu$ M to at most 2.6  $\mu$ M). These plots yielded the bimolecular association rate constant,  $k_{\text{on}}$ , and the overall dissociation rate constant,  $k_{\text{off}}$ , from the slope and ordinate intercept, respectively. Values of  $k_{\text{on}}$  and  $k_{\text{off}}$  for the interaction of the pentasaccharide with most antithrombin variants could be determined in this manner at ionic strengths of both 0.15 and 0.3, but  $k_{\text{off}}$  for the interaction with the N135A variant at ionic strength 0.15 was too low to be experimentally accessible. Instead,  $k_{\text{off}}$  for this interaction was calculated from  $k_{\text{on}}$  and  $K_d$  (Table 1). Values of  $k_{\text{on}}$  and  $k_{\text{off}}$  for the binding of full-length heparin to the variants were only measured at ionic strength 0.3, due to the tight binding at ionic strength 0.15 resulting in  $k_{\text{off}}$  values being too low to be satisfactorily evaluated either experimentally or by calculation.

$k_{\text{on}}$  for the interaction with the pentasaccharide at ionic strength 0.15 was decreased by all substitutions, being  $\sim$ 6-,  $\sim$ 2.5-,  $\sim$ 3-, and  $\sim$ 2-fold lower than that of the N135A

control for the K11A/N135A, K11H/N135A, R13A/N135A, and R24A/N135A variants, respectively (Table 1).  $k_{\text{on}}$  for both pentasaccharide and full-length heparin binding at ionic strength 0.3 was similarly affected by the mutations as pentasaccharide binding at ionic strength 0.15 (Table 1).

All mutations also increased  $k_{\text{off}}$  from that of the N135A control. However, for most mutants, the measured values of  $k_{\text{off}}$  were somewhat, up to  $\sim$ 3-fold, higher than those calculated from  $K_d$  and  $k_{\text{on}}$  (Table 1). Such a discrepancy has also been seen in previous work with other antithrombin variants (21–25) and is most likely due to increased contributions of the preequilibrium pathway of heparin binding to these variants. In the preequilibrium pathway, heparin binds to a small amount of antithrombin that is already conformationally activated and in equilibrium with the unactivated inhibitor (15). A small contribution by this pathway, which is normally negligible as compared with the predominant induced-fit pathway, can result in measured  $k_{\text{off}}$  values being too high without  $k_{\text{on}}$  values being appreciably affected (21). The calculated  $k_{\text{off}}$  values therefore are presumably more correct than the measured ones and were taken to represent the true values. The increase in  $k_{\text{off}}$  for pentasaccharide binding at ionic strength 0.15 was small to moderate for the K11A/N135A, K11H/N135A, and R13A/N135A variants,  $\sim$ 7-,  $\sim$ 2.5-, and  $\sim$ 2-fold, respectively, but appreciably larger,  $\sim$ 25-fold, for the R24A/N135A variant (Table 1). At ionic strength 0.3, the increases in  $k_{\text{off}}$  for binding of both the pentasaccharide and the full-length heparin to the variants in general were slightly lower than for pentasaccharide binding at ionic strength 0.15 (Table 1). However, for both saccharides, the pattern was similar to that observed for the pentasaccharide at the lower ionic strength (i.e., the R24A substitution had the largest effect on  $k_{\text{off}}$ , followed by the K11A substitution).

The heparin concentration dependence of  $k_{\text{obs}}$  for the interaction of the pentasaccharide with the antithrombin variants at ionic strength 0.15 was also analyzed at higher saccharide concentrations. Under these conditions, the resulting plots were hyperbolic (Figure 2), as has been shown previously for the binding of both the pentasaccharide and the full-length heparin to plasma antithrombin and other antithrombin variants (14, 21–25, 35). Such nonlinear behavior is indicative of a two-step binding mechanism, in which a weak interaction with the saccharide is formed in the first step, followed by a conformational change in the second step that increases the binding affinity (eq 1) (13).



In this binding mechanism,  $K_1$  is the dissociation equilibrium constant for the initial weak interaction step, and  $k_{+2}$  and  $k_{-2}$  are the forward and reverse rate constants for the second, conformational change, step. Moreover,  $k_{\text{on}}$  and  $k_{\text{off}}$  are equal to  $k_{+2}/K_1$  and  $k_{-2}$ , respectively. Values of  $K_1$  and  $k_{+2}$  were derived by nonlinear regression fits of the dependence of  $k_{\text{obs}}$  on pentasaccharide concentration to the rectangular hyperbolic function describing the dependence (Figure 2) (13, 14). The K11A substitution increased  $K_1$  for pentasaccharide binding  $\sim$ 2-fold from the value for the N135A control and caused a  $\sim$ 3-fold decrease of  $k_{+2}$  (Table 3). The K11H replacement had an opposite effect on  $K_1$ , decreasing it  $\sim$ 2.5-

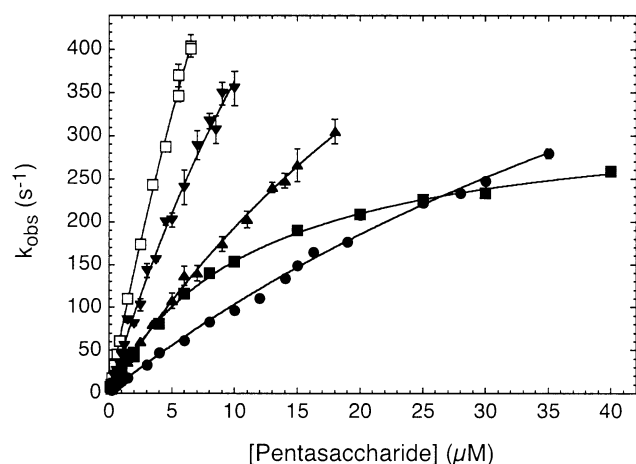


FIGURE 2: Pentasaccharide concentration dependence of observed pseudo-first-order rate constants for pentasaccharide binding to the N135A, K11A/N135A, K11H/N135A, R13A/N135A, and R24A/N135A antithrombin variants at 25 °C, pH 7.4 and ionic strength 0.15. (□) N135A; (●) K11A/N135A; (■) K11H/N135A; (▲) R13A/N135A; and (▼) R24A/N135A. Values are averages  $\pm$  SEM of  $\sim$ 16 individual measurements. Error bars not shown lie within the dimensions of the symbols. The solid lines represent nonlinear regression fits of the data to the rectangular hyperbolic function characterizing the binding mechanism in eq 1 (13, 14). The data for N135A are taken from ref 21.

Table 3: Kinetic Constants for the Two-Step Mechanism of Pentasaccharide Binding to the N135A, K11A/N135A, K11H/N135A, R13A/N135A, and R24A/N135A Antithrombin Variants at 25 °C, pH 7.4 and Ionic Strength 0.15<sup>a</sup>

antithrombin variant	$K_1$ ( $\mu$ M)	$k_{+2}$ ( $s^{-1}$ )	$k_{-2}$ ( $s^{-1}$ )
N135A	$28 \pm 4^b$	$2100 \pm 300^b$	$0.14 \pm 0.07^b$
K11A/N135A	$59 \pm 3$	$680 \pm 30$	$0.95 \pm 0.1$
K11H/N135A	$11 \pm 0.4$	$330 \pm 4$	$0.34 \pm 0.06$
R13A/N135A	$33 \pm 3$	$840 \pm 60$	$0.3 \pm 0.1$
R24A/N135A	$32 \pm 7$	$1500 \pm 300$	$3.2 \pm 0.3$

<sup>a</sup> The dissociation equilibrium constants of the first step,  $K_1$ , and the forward rate constants of the second step,  $k_{+2}$ , were obtained by nonlinear regression fits of the data in Figure 2 to the equation describing the mechanism in eq 1 (13, 14). The reverse rate constants of the second step,  $k_{-2}$ , were taken from Table 1 as the calculated value of  $k_{off}$ . Errors represent the SEM. <sup>b</sup> Taken from ref 21.

fold, and resulted in a larger,  $\sim$ 6-fold, decrease in  $k_{+2}$  than the mutation to Ala (Table 3). The lower  $k_{on}$  values for these two variants than for the control were thus due to altered characteristics of both steps of the binding mechanism. In contrast, the R13A and R24A replacements did not change  $K_1$  and only affected the second step of the interaction, the reduced  $k_{on}$  caused by these substitutions being essentially fully accounted for by decreases in  $k_{+2}$  of  $\sim$ 2.5- and  $<$ 2-fold, respectively (Table 3). All mutations also increased  $k_{-2}$ , which is equal to  $k_{off}$ , to the same extent as the latter parameter (i.e., by  $\sim$ 7-,  $\sim$ 2.5-,  $\sim$ 2-, and  $\sim$ 25-fold for the K11A, K11H, R13A, and R24A mutations, respectively).

**Kinetics of Proteinase Inhibition.** Second-order rate constants for the uncatalyzed and full-length heparin-catalyzed inhibition of thrombin and the uncatalyzed, pentasaccharide-, and full-length heparin-catalyzed inhibition of factor Xa by the K11A/N135A, K11H/N135A, R13A/N135A, and R24A/N135A antithrombin variants were determined at pH 7.4 and ionic strength 0.15. The pentasaccharide enhancement of the rate of thrombin inhibition is less than 2-fold for plasma

antithrombin and the N135A variant (14, 35) and therefore was not investigated. At most, minor effects on the uncatalyzed or catalyzed rate constants for inhibition of thrombin or factor Xa by the antithrombin variants were evident (Table 4).

## DISCUSSION

The N-terminal region of antithrombin is longer and more basic than the corresponding region of other serpins and is considerably flexible (17, 49, 50). This region has been suggested to be important for the binding of heparin from observations that the reduction of the Cys8–Cys128 disulfide bond or cleavage of the Lys29–Ala30 peptide bond leads to decreased heparin affinity (51, 52). Moreover, several individual residues in the N-terminal region have been implicated to participate in heparin binding. Arg24 was originally proposed to be involved in this binding from the identification of a natural human Arg24Cys variant with reduced heparin affinity (32). In apparent contrast to this proposal, the crystal structure of the complex between antithrombin and a synthetic variant of the antithrombin binding heparin pentasaccharide showed that Arg24 is located too far from the latter in the complex to establish any interaction (18). However, the X-ray structure instead suggested two other N-terminal region residues, Lys11 and Arg13, to interact with the pentasaccharide. The importance of Arg13 for the binding was recently supported by the discovery of a natural Arg13Trp antithrombin variant having a decreased heparin affinity (53). The purpose of the present study was to identify the individual contributions of Lys11, Arg13, and Arg24 to heparin binding and to elucidate the apparent discrepancy concerning the role of Arg24 in the interaction. To this end, we expressed recombinant antithrombin variants with Lys11Ala, Lys11His, Arg13Ala, and Arg24Ala substitutions on an Asn135Ala background in a baculovirus expression system. The resulting variants all had reduced heparin affinities that were similar for pentasaccharide and full-length heparin, indicating that the three N-terminal residues are important for binding the specific pentasaccharide region of the polysaccharide. All variants showed normal tryptophan fluorescence enhancement on heparin binding and normal uncatalyzed and heparin-catalyzed rate constants for inhibition of thrombin and factor Xa. These observations imply that the substitutions only affected the heparin affinity of antithrombin without altering the overall conformation of the native or heparin-activated protein, as was also the case in our previous studies of other recombinant antithrombin variants (21–25, 35, 47).

Substitution of Lys11 by the shorter and noncharged Ala decreased the affinity of antithrombin for the heparin pentasaccharide  $\sim$ 40-fold at physiological pH and ionic strength. This affinity decrease corresponds to a loss in binding energy of approximately  $-9$  kJ mol<sup>-1</sup> (i.e.,  $\sim$ 18% of the total free energy of binding of the pentasaccharide to the antithrombin control). Lys11 is thus of appreciable importance for pentasaccharide binding, being responsible for maintaining comparable binding energy as Arg47, although less than Lys114, Lys125, or Arg129 (21–24). The reduced affinity was due to the loss of approximately one ionic interaction, consistent with the mutation abolishing one positive charge, as well as to a  $\sim$ 3-fold decrease in affinity



Table 4: Association Rate Constants for Uncatalyzed and Pentasaccharide- or Full-Length Heparin-Catalyzed Inhibition of Proteinases by the N135A, K11A/N135A, K11H/N135A, R13A/N135A, and R24A/N135A Antithrombin Variants at 25 °C, pH 7.4 and Ionic Strength 0.15<sup>a</sup>

proteinase	antithrombin variant	$k_{\text{uncat}}$ ( $\times 10^3 \text{ M}^{-1} \text{ s}^{-1}$ )	$k_{\text{H5}}$ ( $\times 10^5 \text{ M}^{-1} \text{ s}^{-1}$ )	$k_{\text{H26}}$ ( $\times 10^6 \text{ M}^{-1} \text{ s}^{-1}$ )
thrombin	N135A	$9.4 \pm 0.4^b$	nd <sup>c</sup>	$9.0 \pm 0.5^b$
	K11A/N135A	$10 \pm 0.1$	nd	$12 \pm 1$
	K11H/N135A	$13 \pm 2$	nd	$15 \pm 1$
	R13A/N135A	$10 \pm 0.1^d$	nd	$11 \pm 0.9$
	R24A/N135A	$9.6 \pm 0.2$	nd	$11 \pm 1$
factor Xa	N135A	$4.8 \pm 0.2^b$	$6.1 \pm 0.2^b$	$1.2 \pm 0.04^b$
	K11A/N135A	$4.9 \pm 0.3$	$4.9 \pm 0.3$	$0.80 \pm 0.09$
	K11H/N135A	$5.8 \pm 0.8$	$4.8 \pm 0.1$	$2.0 \pm 0.1$
	R13A/N135A	$6.7 \pm 0.1$	$6.0 \pm 0.6$	$1.5 \pm 0.1$
	R24A/N135A	$4.8 \pm 0.1$	$6.8 \pm 1.3$	$1.5 \pm 0.1$

<sup>a</sup> Second-order association rate constants for uncatalyzed ( $k_{\text{uncat}}$ ), pentasaccharide-catalyzed ( $k_{\text{H5}}$ ), and full-length heparin-catalyzed ( $k_{\text{H26}}$ ) reactions of the antithrombin variants with proteinases were determined as described in the Materials and Methods. Uncatalyzed rate constants are averages  $\pm$  SEM of at least three determinations. Values of  $k_{\text{H5}}$  and  $k_{\text{H26}} \pm$  SEM were obtained by linear regression of plots of  $k_{\text{obs}}$  vs the concentration of the antithrombin–saccharide complex, comprising four to five points in the 0–8 nM concentration range. Complex concentrations were calculated from  $K_d$  values at ionic strength 0.15 that were either measured directly, or in the case of full-length heparin binding to the K11A, K11H, or R13A variants, were estimated from the measured  $K_d$  at ionic strength 0.3 together with the ionic-strength dependence of  $K_d$  for pentasaccharide binding.

<sup>b</sup> Taken from ref 21. <sup>c</sup> Not determined. <sup>d</sup> Measured in the presence of 50  $\mu\text{g/mL}$  polybrene. In the absence of polybrene, the measured rate constant was 1.2-fold higher, indicating a minor heparin contamination, corresponding to a molar ratio to antithrombin of less than 0.001. Since polybrene appreciably (15–30%) enhances the rate of antithrombin–factor Xa reaction, the corresponding rate constant for factor Xa was measured with a further purified preparation of the R13A/N135A antithrombin variant. The uncatalyzed rate constants for the K11A/N135A, K11H/N135A, and R24A/N135A variants were unaffected by the presence of polybrene, indicating that no heparin contamination was present.

of nonionic interactions (i.e., hydrogen bonds, van der Waal's bonds, and hydrophobic interactions). Lys11 thus provides both ionic and nonionic interactions with the pentasaccharide. Rapid kinetics analyses showed that the Lys11Ala variant had a  $\sim 2$ -fold higher dissociation equilibrium constant of the first step of the two-step mechanism of pentasaccharide binding to antithrombin than the control inhibitor, indicating that Lys11 is involved in the initial recognition of the pentasaccharide. Lys125 has previously been shown to be of primary importance for this recognition step (24). Both the Lys11 and the Lys125 side chains are directed toward the same region in the X-ray structure of free antithrombin and also interact with the same carboxylate group of the E unit of the pentasaccharide in the X-ray crystal structure of the antithrombin–pentasaccharide complex (Figure 3A, B) (17, 18). These two regions of antithrombin and the pentasaccharide therefore presumably are important for the first contact between the two reactants to be established. The involvement of the E residue of the pentasaccharide in the initial recognition is in agreement with a previously proposed mechanism of pentasaccharide binding (15). In addition to affecting the first step of pentasaccharide binding, the Lys11Ala substitution also caused a small reduction in the forward rate constant and a somewhat larger increase in the reverse rate constant of the second step. Lys11 is therefore of importance both for inducing the conformational change of antithrombin on binding of the pentasaccharide and for locking the antithrombin–pentasaccharide complex in the activated state. Like Lys125, Lys11 thus participates in both pentasaccharide binding steps, although it is of less importance for both these steps than the former residue (24). Cleavage of the neighboring Cys8–Cys128 disulfide bond may primarily perturb these interactions of Lys11 with the pentasaccharide, accounting for the decreased heparin affinity resulting from such cleavage (51).

Replacement of Lys11 by His, which is more polar and more similar in size to Lys than Ala, resulted in a  $\sim 6$ -fold reduction of pentasaccharide affinity at physiological pH and ionic strength, appreciably less than the decrease caused by

the substitution to Ala. The Lys11 to His replacement caused the loss of approximately one ionic interaction at pH 7.4, like the Ala substitution, but in no loss of nonionic interactions. The His side chain can thus provide nonionic interactions with the pentasaccharide of comparable strength as Lys11, accounting for the lower decrease in overall affinity caused by the His mutation. The finding that the Lys11His substitution resulted in no loss of ionic interactions at pH 6, where the His side chain is positively charged, indicates that the positive charge at position 11 necessary for optimal interaction with the pentasaccharide is not specific for a Lys side chain. In contrast to the mutation of Lys 11 to Ala, which results in nearly total removal of the Lys side chain, replacement of this residue with His increased the affinity of the first step of pentasaccharide binding at pH 7.4  $\sim 2.5$ -fold from that of the control, in addition to moderately affecting both rate constants of the second step. This higher affinity of the initial recognition step may be due to the nonionic interactions provided by the His side chain being established to a larger extent in the first step, and consequently to a lower extent in the second step, than those provided by the Lys side chain.

The Arg13 to Ala antithrombin variant had only a  $\sim 7$ -fold lower affinity for the pentasaccharide than the control, corresponding to a loss in binding energy of approximately  $-5 \text{ kJ mol}^{-1}$  (i.e.,  $\sim 10\%$  of the total free energy of pentasaccharide binding). Arg13 is thus of only modest importance for this binding, appreciably less so than Lys11. The decreased affinity was due to the loss of one ionic interaction, whereas the nonionic interactions were unaffected, indicating that Arg13 only participates in the binding by its positive charge. The Arg13Ala substitution did not affect the initial recognition of the pentasaccharide but moderately affected both the forward and the reverse rate constants of the second, conformational change step. The ionic interaction provided by Arg13 is thus involved only in the second step of pentasaccharide binding, contributing somewhat both to the induced conformational change and to keeping the saccharide anchored to the activated inhibitor.

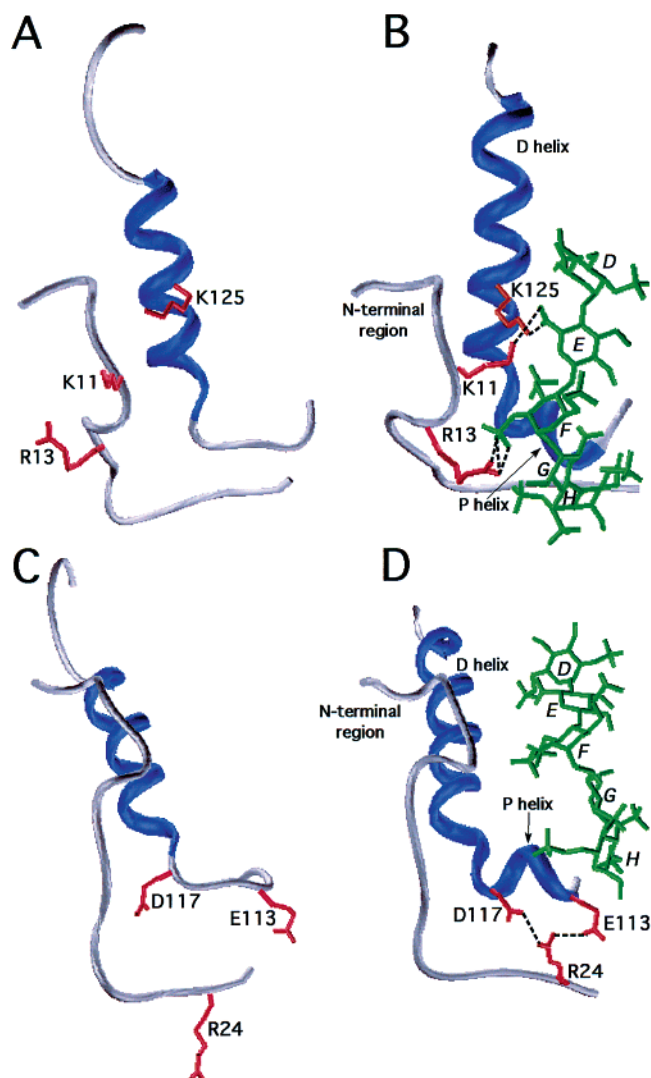


FIGURE 3: Close-up of the heparin binding site of antithrombin. (A and B) Interactions involving Lys11 and Arg13 and (C and D) interactions involving Arg24. (A and C) Free antithrombin and (B and D) pentasaccharide-bound antithrombin. Antithrombin residues 6–25 and 111–136, located in and around the N-terminal region and the D- and P-helices, are shown. Helix structures are in blue and coil structures in gray. The side-chains of Lys11, Arg13, Arg24, Glu113, Asp117, and Lys125 are drawn in red. The pentasaccharide, denoted DEFGH from the nonreducing end, is shown in green. Dotted lines represent proposed interactions with distances  $<\sim 3$  Å. Drawn from PDB structures 1E03 and 1E05 (17, 18).

The crystal structure of the antithrombin–pentasaccharide complex indicates that this ionic interaction is to the 2-*N*-sulfate group on the F-unit of the natural heparin pentasaccharide (Figure 3A,B) (18).

Substitution of Arg24 by Ala resulted in a similar  $\sim 40$ -fold reduced affinity for the pentasaccharide as the Lys11Ala mutation, corresponding to a decrease in binding energy of approximately  $-9$  kJ mol $^{-1}$  (i.e.,  $\sim 18\%$  of the total binding energy). Arg24 and Lys11 are thus of comparable importance for pentasaccharide binding. The lower affinity was due to the loss of one ionic interaction as well as to a  $\sim 5$ -fold decrease in the strength of nonionic interactions, indicating that Arg24 is responsible for maintaining both types of interactions with the pentasaccharide. These interactions must be made exclusively in the second binding step, as the dissociation equilibrium constant of the first step was

unaffected by the mutation. Moreover, the role of the interactions in the second step is primarily to stabilize the pentasaccharide-induced activated state of antithrombin, as evidenced by the substantial,  $\sim 25$ -fold, increased reverse rate constant of this step caused by the substitution. Although Arg24 does not interact directly with the pentasaccharide in the X-ray structure of the antithrombin–pentasaccharide complex (18), these observations can nevertheless be satisfactorily interpreted from this structure. In the complex, Arg24 is seen to interact with two other antithrombin residues, Glu113 and Asp117, located in the region at the base of the D-helix, which rearranges to form the short P-helix on pentasaccharide binding (Figure 3C,D). In contrast, these interactions are not made in free antithrombin, in which this region is more unstructured. The role of Arg24 in pentasaccharide binding thus appears to be to stabilize the P-helix, which is formed as an essential component of the pentasaccharide-induced conformational change (17, 18). Its creation serves primarily to position the pivotal Lys114 residue, which contributes most of all antithrombin residues studied so far to the pentasaccharide-induced conformational change (23), for optimal binding to the saccharide. The losses of ionic and nonionic interactions with the pentasaccharide and the resulting loss in overall affinity observed on mutation of Arg 24 are therefore most likely due to alterations of the interactions involving Lys114. Cleavage of the neighboring Lys29–Ala30 peptide bond would be expected to affect the ability of Arg24 to stabilize the P-helix. Consequently, this cleavage would change the mode of interaction of Lys114 with the pentasaccharide, leading to the observed increased dissociation rate constant and decreased affinity of heparin binding (52).

The three N-terminal region residues characterized in this work appear to act noncooperatively in pentasaccharide binding, as the mutations, which each abolished one positive charge, also each resulted in the loss of one ionic interaction on pentasaccharide binding. This behavior is similar to that of Arg47 but in contrast to that of the three antithrombin residues contributing most to heparin affinity, Lys114, Lys125, and Arg129, which were found to act cooperatively in the binding (21–24). This cooperativity accounts for the finding that the sum of the losses in pentasaccharide binding energy caused by mutation of the different antithrombin residues substantially exceeds the total binding energy (5).

In conclusion, the N-terminal region of antithrombin is critical for high-affinity pentasaccharide binding, being involved in both the initial recognition of the saccharide in the first binding step and the induction and stabilization of the induced conformational change in the second step. Lys11 and Arg24 in this region are responsible for maintaining a similar overall binding energy, whereas Arg13 is less important. Lys11 is the only one of the three residues that participates in recognizing the heparin pentasaccharide in the initial complex. Lys11, Arg13, and Arg24 subsequently all aid in promoting the conformational change and stabilizing the high-affinity complex by a substantial rearrangement of their side chains (Figure 3). Lys11 and Arg13 interact directly with the pentasaccharide by providing ionic, and in the case of Lys11 also nonionic, interactions. In contrast, Arg24 is of importance for the stabilization of the complex by forming intramolecular ionic and nonionic interactions with Glu113 and Asp117, located in the pentasaccharide-induced P-helix.



Collectively, these results illustrate how contact and non-contact residues participating in a protein–ligand interaction can play very different roles in the energetics and dynamics of binding of the ligand and in the conformational changes induced by this binding.

## ACKNOWLEDGMENT

We thank Yancheng Zuo and Aiqin Lu for production and initial purification of the antithrombin variants and Richard Swanson for assistance in the analyses of the K11 mutants.

## REFERENCES

- Ishiguro, K., Kojima, T., Kadamatsu, K., Nakayama, Y., Takagi, A., Suzuki, M., Takeda, N., Ito, M., Yamamoto, K., Matsushita, T., Kusugami, K., Muramatsu, T., and Saito, H. (2000) *J. Clin. Invest.* **106**, 873–878.
- Gettins, P. G. W., Patston, P. A., and Olson, S. T. (1996) in *Serpins: Structure, Function and Biology*, R. G. Landes, Austin, TX.
- Björk, I., and Olson, S. T. (1997) in *Chemistry and Biology of Serpins* (Church, F. C., Cunningham, D. D., Ginsburg, D., Hoffman, M., Stone, S. R., and Tollefsen, D. M., Eds.) pp 17–33, Plenum Press, New York.
- Van Boven, H. H. and Lane, D. A. (1997) *Semin. Hematol.* **34**, 188–204.
- Olson, S. T., Björk, I., and Bock, S. C. (2002) *Trends Cardiovasc. Med.* **12**, 198–205.
- Bedsted, T., Swanson, R., Chuang, Y.-J., Bock, P. E., Björk, I., and Olson, S. T. (2003) *Biochemistry* **42**, 8143–8152.
- Gettins, P. G. W. (2002) *Chem. Rev.* **102**, 4751–4803.
- Stratikos, E., and Gettins, P. G. W. (1999) *Proc. Natl. Acad. Sci. U.S.A.* **96**, 4808–4813.
- Lawrence, D. A., Olson, S. T., Muhammad, S., Day, D. E., Kvassman, J. O., Ginsburg, D., and Shore, J. D. (2000) *J. Biol. Chem.* **275**, 5839–5844.
- Huntington, J. A., Read, R. J., and Carrell, R. W. (2000) *Nature* **407**, 923–926.
- Calugaru, S. V., Swanson, R., and Olson, S. T. (2001) *J. Biol. Chem.* **276**, 32446–32455.
- Olson, S. T., and Björk, I. (1994) *Semin. Thromb. Hemost.* **20**, 373–409.
- Olson, S. T., Srinivasan, K. R., Björk, I., and Shore, J. D. (1981) *J. Biol. Chem.* **256**, 11073–11079.
- Olson, S. T., Björk, I., Sheffer, R., Craig, P. A., Shore, J. D., and Choay, J. (1992) *J. Biol. Chem.* **267**, 12528–12538.
- Desai, U. R., Petitou, M., Björk, I., and Olson, S. T. (1998) *J. Biol. Chem.* **273**, 7478–7487.
- Desai, U. R., Petitou, M., Björk, I., and Olson, S. T. (1998) *Biochemistry* **37**, 13033–13041.
- Skinner, R., Abrahams, J. P., Whisstock, J. C., Lesk, A. M., Carrell, R. W., and Wardell, M. R. (1997) *J. Mol. Biol.* **266**, 601–609.
- Jin, L., Abrahams, J. P., Skinner, R., Petitou, M., Pike, R. N., and Carrell, R. W. (1997) *Proc. Natl. Acad. Sci. U.S.A.* **94**, 14683–14688.
- Huntington, J. A., McCoy, A., Belzar, K. J., Pei, X. Y., Gettins, P. G. W., and Carrell, R. W. (2000) *J. Biol. Chem.* **275**, 15377–15383.
- Chuang, Y. J., Swanson, R., Raja, S. M., and Olson, S. T. (2001) *J. Biol. Chem.* **276**, 14961–14971.
- Arocas, V., Bock, S. C., Olson, S. T., and Björk, I. (1999) *Biochemistry* **38**, 10196–10204.
- Desai, U., Swanson, R., Bock, S. C., Björk, I., and Olson, S. T. (2000) *J. Biol. Chem.* **275**, 18976–18984.
- Arocas, V., Bock, S. C., Raja, S., Olson, S. T., and Björk, I. (2001) *J. Biol. Chem.* **276**, 43809–43817.
- Schedin-Weiss, S., Desai, U. R., Bock, S. C., Gettins, P. G. W., Olson, S. T., and Björk, I. (2002) *Biochemistry* **41**, 4779–4788.
- Schedin-Weiss, S., Arocas, V., Bock, S. C., Olson, S. T., and Björk, I. (2002) *Biochemistry* **41**, 12369–12376.
- Turpie, A. G. G., Gallus, A. S., and Hoek, J. A. (2001) *N. Engl. J. Med.* **344**, 619–625.
- Eriksson, B. I., Bauer, K. A., Lassen, M. R., and Turpie, A. G. G. (2001) *N. Engl. J. Med.* **345**, 1298–1304.
- Bauer, K. A., Eriksson, B. I., Lassen, M. R., and Turpie, A. G. G. (2001) *N. Engl. J. Med.* **345**, 1305–1310.
- HajMohammadi, S., Enjyoji, K., Princivalle, M., Christi, P., Lech, M., Beeler, D., Rayburn, H., Schwartz, J. J., Barzegar, S., De Agostini, A. I., Post, M. J., Rosenberg, R. D., and Shworak, N. W. (2003) *J. Clin. Invest.* **111**, 989–999.
- Marcum, J. A., Atha, D. H., Fritze, L. M., Nawroth, P., Stern, D., and Rosenberg, R. D. (1986) *J. Biol. Chem.* **261**, 7507–7517.
- De Agostini, A. I., Watkins, S. C., Slayter, H. S., Youssoufian, H., and Rosenberg, R. D. (1990) *J. Cell Biol.* **111**, 1293–1304.
- Borg, J. Y., Brennan, S. O., Carrell, R. W., George, P., Perry, D. J., and Shaw, J. (1990) *FEBS Lett.* **266**, 163–166.
- Ersdal-Badju, E., Lu, A., Peng, X., Picard, V., Zendehrouh, P., Turk, B., Björk, I., Olson, S. T., and Bock, S. C. (1995) *Biochem. J.* **310**, 323–330.
- Ersdal-Badju, E., Lu, A. Q., Zuo, Y. C., Picard, V., and Bock, S. C. (1997) *J. Biol. Chem.* **272**, 19393–19400.
- Turk, B., Brieditis, I., Bock, S. C., Olson, S. T., and Björk, I. (1997) *Biochemistry* **36**, 6682–6691.
- Laemmli, U. K. (1970) *Nature* **227**, 680–685.
- Schägger, H., and von Jagow, G. (1987) *Anal. Biochem.* **166**, 368–379.
- Nordenman, B., Nyström, C., and Björk, I. (1977) *Eur. J. Biochem.* **78**, 195–203.
- Bock, P. E., Craig, P. A., Olson, S. T., and Singh, P. (1989) *Arch. Biochem. Biophys.* **273**, 375–388.
- Choay, J., Petitou, M., Lormeau, J. C., Sinay, P., Casu, B., and Gatti, G. (1983) *Biochem. Biophys. Res. Commun.* **116**, 492–499.
- Olson, S. T., and Björk, I. (1991) *J. Biol. Chem.* **266**, 6353–6364.
- Olson, S. T., Björk, I., and Shore, J. D. (1993) *Methods Enzymol.* **222**, 525–560.
- Björk, I., Ylinenjärvi, K., Olson, S. T., Hermentin, P., Conradt, H. S., and Zettlmeissl, G. (1992) *Biochem. J.* **286**, 793–800.
- Picard, V., Ersdal-Badju, E., and Bock, S. C. (1995) *Biochemistry* **34**, 8433–8440.
- Fan, B., Crews, B. C., Turko, I. V., Choay, J., Zettlmeissl, G., and Gettins, P. (1993) *J. Biol. Chem.* **268**, 17588–17596.
- Garone, L., Edmunds, T., Hanson, E., Bernasconi, R., Huntington, J. A., Meagher, J. L., Fan, B. Q., and Gettins, P. G. W. (1996) *Biochemistry* **35**, 8881–8889.
- Arocas, V., Turk, B., Bock, S. C., Olson, S. T., and Björk, I. (2000) *Biochemistry* **39**, 8512–8518.
- Record, M. T., Jr., Lohman, T. M., and de Haseth, P. (1976) *J. Mol. Biol.* **107**, 145–158.
- Carrell, R., and Travis, J. (1985) *Trends Biochem. Sci.* **10**, 20–24.
- Huber, R., and Carrell, R. W. (1989) *Biochemistry* **28**, 8951–8966.
- Sun, X. J., and Chang, J. Y. (1989) *J. Biol. Chem.* **264**, 11288–11293.
- Fitton, H. L., Skinner, R., Dafforn, T. R., Jin, L., and Pike, R. N. (1998) *Protein Sci.* **7**, 782–788.
- Picard, V., Susen, S., Bellucci, S., Aiach, M., and Alhenc-Gelas, M. (2003) *J. Thromb. Haemost.* **1**, 386–387.

BI030173B